AD-A105 873 ORINCON CORP LA JOLLA CA F/G 9/4
ADAPTIVE ENHANCEMENT OF FINITE BANDWIDTH SIGNALS IN WHITE GAUSS--ETC(U)
AUG 81 C M ANDERSON, E H SATORIUS N66001-79-C-0204
UNCLASSIFIED NOSC-TR-711 NL

1 OF 1
AD A 105 873

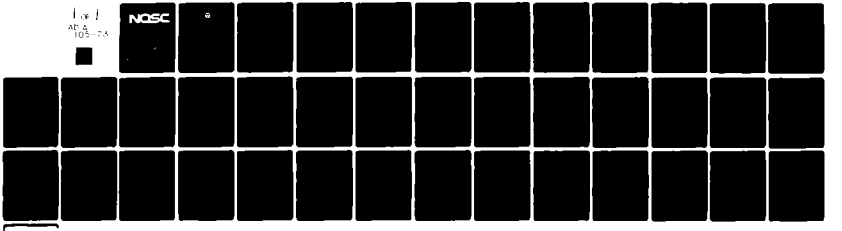

END
DATE FILMED
11-81
DTIC

NOSC

NOSC TR 711

NOSC TR 711

Technical Report 711

ADAPTIVE ENHANCEMENT OF FINITE BANDWIDTH SIGNALS IN WHITE GAUSSIAN NOISE

C.M. Anderson
Orincon Corporation
N66001-79-C-0204

E.H. Satorius
J.R. Zeidler
NOSC

15 August 1981

Final Report: January 1979 - June 1981

Prepared for
Naval Electronic Systems Command
Naval Sea Systems Command

Approved for public release; distribution unlimited

NAVAL OCEAN SYSTEMS CENTER
SAN DIEGO, CALIFORNIA 92152

NAVAL OCEAN SYSTEMS CENTER, SAN DIEGO, CA 92152

AN ACTIVITY OF THE NAVAL MATERIAL COMMAND

SL GUILLE, CAPT, USN
Commander

HL BLOOD
Technical Director

ADMINISTRATIVE INFORMATION

Work for this report was performed from January 1979 to June 1981 under funds provided by NAVELEX 320 and NAVSEA 63Y1. Program elements 62711N and 63553N, project numbers F11101 and S0229-AS, and task area XF111-011-00 were assigned to the project.

E. H. Satorius is presently employed by Dynamics Technology, Inc., although he was a NOSC employee when he contributed to this report. C. M. Anderson works for ORINCON Corporation and co-authored this report under contract N66001-79-C-0204.

Reviewed by
P. M. REEVES, Head
Electronics Division

Under authority of
R. H. HEARN, Head
Fleet Engineering Department

UNCLASSIFIED

SECURITY CLASSIFICATION OF THIS PAGE (When Data Entered)

REPORT DOCUMENTATION PAGE

READ INSTRUCTIONS BEFORE COMPLETING FORM

1. REPORT NUMBER: NOSC Technical Report 711 (TR 711)	2. GOVT ACCESSION NO.: AD-A105873
3. RECIPIENT'S CATALOG NUMBER:	
4. TITLE (and Subtitle): ADAPTIVE ENHANCEMENT OF FINITE BANDWIDTH SIGNALS IN WHITE GAUSSIAN NOISE	5. TYPE OF REPORT & PERIOD COVERED: Final Report: January 1979 - June 1981
	6. PERFORMING ORG. REPORT NUMBER:
7. AUTHOR(s): C. M. Anderson (ORINCON); E. H. Satorius; J. R. Zeidler (NOSC)	8. CONTRACT OR GRANT NUMBER(s): N66001-79-C-0204
9. PERFORMING ORGANIZATION NAME AND ADDRESS: Naval Ocean Systems Center, San Diego, CA 92152	10. PROGRAM ELEMENT, PROJECT, TASK AREA & WORK UNIT NUMBERS: 62711N-F11101-XF111-011-00; 63553N, S0229-AS
11. CONTROLLING OFFICE NAME AND ADDRESS: Naval Electronic Systems Command and Naval Sea Systems Command, Washington, DC 20360	12. REPORT DATE: 15 August 1981
	13. NUMBER OF PAGES: 34
14. MONITORING AGENCY NAME & ADDRESS (if different from Controlling Office)	15. SECURITY CLASS. (of this report): Unclassified
	15a. DECLASSIFICATION DOWNGRADING SCHEDULE

16. DISTRIBUTION STATEMENT (of this Report)

Approved for public release; distribution unlimited.

17. DISTRIBUTION STATEMENT (of the abstract entered in Block 20, if different from Report)

18. SUPPLEMENTARY NOTES

19. KEY WORDS (Continue on reverse side if necessary and identify by block number)

Adaptive filtering
Adaptive line enhancement
Linear prediction filtering
Detection
Signal Bandwidth

20. ABSTRACT (Continue on reverse side if necessary and identify by block number)

The steady-state behavior of the adaptive line enhancer (ALE) is analyzed for stationary inputs consisting of finite bandwidth signals embedded in a white Gaussian noise (WGN) background. Analytic expressions for the weights and output of the LMS adaptive filter are derived as functions of input signal bandwidth and SNR, as well as ALE length and bulk delay. The steady-state gain in broadband SNR from input to output is derived as a function of these same four variables. For fixed ALE parameters and input SNR, it is shown that this gain increases as the input signal becomes narrower and approaches the sinusoidal limit. It is emphasized that because the correlation time of finite bandwidth signals is limited, excessively large values of the ALE bulk delay parameter result in diminished gain. Furthermore, there is an optimal filter length, whose value depends upon signal bandwidth and SNR, for which the

DD FORM 1 JAN 73 1473 EDITION OF 1 NOV 65 IS OBSOLETE

S N 0102-LF-014-6601

UNCLASSIFIED

SECURITY CLASSIFICATION OF THIS PAGE (When Data Entered)

20. ABSTRACT: (Continued)

broadband gain is maximized. These results demonstrate the importance of including the effects of algorithm noise in analyzing the performance of real-time adaptive processors.

SUMMARY

The steady-state behavior of the adaptive line enhancer (ALE) is analyzed for stationary inputs consisting of finite bandwidth signals embedded in a white Gaussian noise (WGN) background. Analytic expressions for the weights and output of the LMS adaptive filter are derived as functions of input signal bandwidth and SNR, as well as ALE length and bulk delay. The steady-state gain in broadband SNR from input to output is derived as a function of these same four variables. For fixed ALE parameters and input SNR, it is shown that this gain increases as the input signal becomes narrower and approaches the sinusoidal limit. It is emphasized that because the correlation time of finite bandwidth signals is limited, excessively large values of the ALE bulk delay parameter result in diminished gain. Furthermore, there is an optimal filter length, whose value depends upon signal bandwidth and SNR, for which the broadband gain is maximized. These results demonstrate the importance of including the effects of algorithm noise in analyzing the performance of real-time adaptive processors.

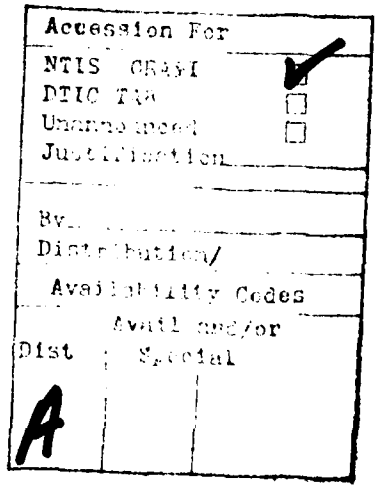

CONTENTS

1.0 INTRODUCTION

Adaptive digital filtering techniques have been shown to be effective in a wide range of practical applications where there is insufficient a priori knowledge of the expected signal and noise parameters to design optimal fixed filters. The increased computational speed and performance capabilities of modern digital hardware has made it possible to apply adaptive filtering techniques in a wide range of applications in recent years. Representative applications include noise cancellation [1], bioengineering [1], echo cancellation [2,3], data equalization [4-6], predictive deconvolution [7], instantaneous frequency tracking [8-10], speech processing [1,11-13], environmental prediction [14], intrusion detection [15,16], beamforming [17-19], radar clutter rejection [20], data communications [21,22], systems identification [23,24], narrowband signal enhancement [1,10,25-27], narrowband signal detection [28,29], coherence detection [30], spectral estimation [25,31,32], and narrowband interference rejection [33].

Many of the above applications employ external noise references to remove noise contamination from a desired signal as discussed in [1]. In applications where an external reference for the additive noise is not available, the interfering noise may be suppressed using a Wiener linear prediction filter (LPF) if there is a significant difference in the bandwidth of the signal and the additive noise [1,25-33]. As discussed in the above references, a variety of adaptive estimation techniques have been employed to provide time-varying estimates of the Wiener filter coefficients. These include finite impulse response (FIR), infinite impulse response (IIR), and adaptive lattice algorithms. The estimation technique which is most commonly employed in real-time applications is the Widrow-Hoff Least Mean Squares (LMS) adaptive algorithm. (In fact, echo cancellers which utilize a 128 tap LMS FIR digital adaptive filter are now being produced on a single silicon integrated circuit chip [34]). In this paper, the steady-state performance of an adaptive LPF which employs the LMS adaptive algorithm to estimate the Wiener filter coefficients

will be analyzed under specified stationary input conditions. This implementation is the adaptive line enhancer (ALE) which is discussed in references [1,10,25-33]. As indicated in Figure 1, the ALE is a digital Δ-step linear prediction filter for which f_s is the sample rate, L is the number of adaptive weights, and Δ is a bulk delay of an integral number of samples. For narrowband enhancement applications, the output is r(k)*, and Δ is chosen to optimize the frequency resolution as discussed in [25,31,32]. In the case of finite bandwidth signals in correlated noise, Δ is selected so as to suppress the additive noise without causing significant signal attenuation [35].

References [1-33] contain a variety of applications of adaptive Wiener LPFs. As discussed in [23], the accuracy of FIR system identification methods is dependent upon the input signal to noise ratio (SNR) and the bandwidth of the input signal(s) of interest. Effective utilization of adaptive LPF techniques for single reference noise suppression applications requires knowledge of the values of Δ and L that maximize noise suppression without appreciable signal distortion. The elimination of signal distortion is particularly important for the application of LPF methods to speech enhancement [12,13], system identification [23,24], and other applications described in [1-33]. It was shown in [25] that the LPF produces an intrinsic amplitude distortion which is a function of the input SNR for sinusoidal signals embedded in uncorrelated noise. The gain in output SNR of the ALE relative to that of the input was shown to be dependent on the input SNR and is limited by the algorithm noise of the LMS estimation algorithm [26]. It was demonstrated in [29] that the statistical properties of the input are significantly altered by the ALE.

---

*By using the error signal $\varepsilon(k)$ as the output of the device, the ALE can also be applied to the suppression of narrowband interference from broadband signals of interest.

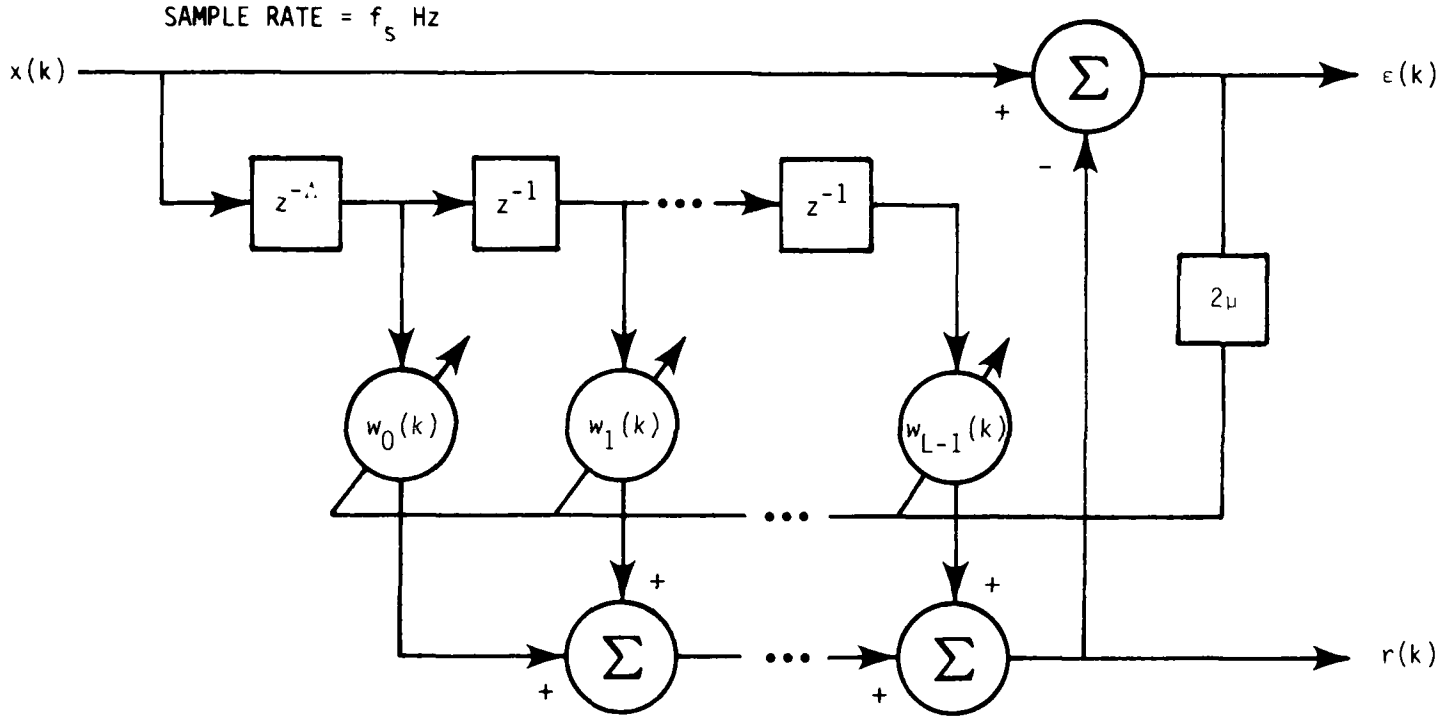

Figure 1. Block diagram of the ALE where weights $w_i(k)$ are updated in accordance with the Widrow-Hoff algorithm $w_i(k+1) = w_i(k) + 2\mu\varepsilon(k)\,x(k-i-\Delta)$.

In this paper we will extend the results obtained in [25,26] to derive analytical expressions for the impulse response and transfer function of a Wiener LPF and for the output power spectral density of the ALE for an input signal composed of one or more stationary narrowband signals in white Gaussian noise (WGN). These signals consist of WGN passed through a filter whose bandwidth α is quite small relative to the Nyquist frequency, but generally comparable to the bin width 1/L. Analytical expressions for the LPF impulse response and transfer function will be developed assuming a stationary input sequence x(k) whose autocorrelation function is known exactly and has a rational z-transform, $S_{xx}(z)$. Under these conditions, the solution for the FIR Wiener LPF impulse response may be obtained by using the method of undetermined coefficients to solve a set of linear equations in which the dimensionality is reduced from L to a value determined by the number of poles and zeroes of $S_{xx}(z)$. As discussed in [36,37], the use of methods such as Levinson's algorithm provides efficient computational techniques for solving the L dimensional Wiener equations but requires the number of filter taps and the prediction distance to be known explicitly. The formulation used in this paper allows L and Δ to be treated as adjustable design parameters whose values can be chosen so as to maximize output SNR for various input conditions. These results illustrate that the Wiener LPF will produce both amplitude and bandwidth distortion of the narrowband components of x(k) at the filter output y(k). It will further be shown that the magnitude of this distortion is a function of the input SNR, the bandwidth (α) of the signal, and the frequency resolution (f_s/L) of the LPF. These results reduce to those previously derived for sinusoidal inputs in [25] when $\alpha = 0$.

The steady-state noise suppression capabilities of the ALE will be determined as a function of the input signal bandwidth and the input SNR for a single bandlimited input in WGN. Analytic expressions will be derived which express the impulse response and transfer function of the ideal Wiener LPF as a function of both filter parameters and

signal variables. Using a definition of output SNR that considers contributions of both the optimal Wiener filter and the misadjustment noise of the LMS algorithm, broadband gain will be computed as a function of the ALE parameters L, Δ, and the feedback gain constant μ, as well as the input variables α and SNR. It will be demonstrated that for ALE parameters and broadband input SNR fixed, the gain of the device decreases as the input signal bandwidth increases. In addition, Δ should not exceed $1/\alpha$, and there is an optimal value of L which is a function of the input signal bandwidth and broadband SNR. In the limit as $\alpha \to 0$, these results are found to be in agreement with those of previous studies dealing with sinusoidal signals embedded in a WGN background.

2.0 ALE WEIGHT-VECTOR MODEL

The basic properties of the adaptive line enhancer and its operation are described in [1,25,26]. As indicated by the block diagram in Figure 1, the ALE consists of an L-weight linear prediction filter in which the filter coefficients, $w_i(k)$, are updated at the input sampling rate, f_s. The adaptive filter output $r(k)$ is defined by

$$r(k) = \sum_{i=0}^{L-1} w_i(k)\, x(k-i-\Delta), \tag{1}$$

where Δ is the prediction distance of the filter measured in samples. The output $r(k)$ is then subtracted from the input sequence $x(k)$ to form an error sequence $\varepsilon(k)$. The error sequence is multiplied by a scalar constant, μ, and fed back to adjust the filter weights according to the Widrow-Hoff LMS algorithm [38]

$$w_i(k+1) = w_i(k) + 2\mu\varepsilon(k)\, x(k-i-\Delta), \quad i = 0,1,\ldots,L-1. \tag{2}$$

Provided that the feedback constant μ is strictly less than the reciprocal of the largest eigenvalue of the input autocorrelation matrix, the expected value of the weight vector $\underline{w}(k)$ converges to the Wiener solution

$$\underline{w}^* = \Phi^{-1}\,\underline{d} \tag{3}$$

where Φ is the L×L input data autocorrelation matrix with elements $\Phi_{k,\ell} = \phi_{xx}(k-\ell) = E\{x(k)\,\overline{x(\ell)}\}$ and $\underline{d}$ is a vector of length L with components $d_k = \phi_x(k+\Delta)$.

As developed in prior work [26] and depicted in Figure 2, a steady-state model for the converged ALE weight vector $\underline{w}(k) = [w_0(k) \ \ldots \ w_{L-1}(k)]^T$ may be obtained by decomposing $\underline{w}(k)$ into two parallel weight vectors $\underline{w}(k) = \underline{w}^* + \hat{\underline{w}}(k)$. Here, $\underline{w}^*$ is the

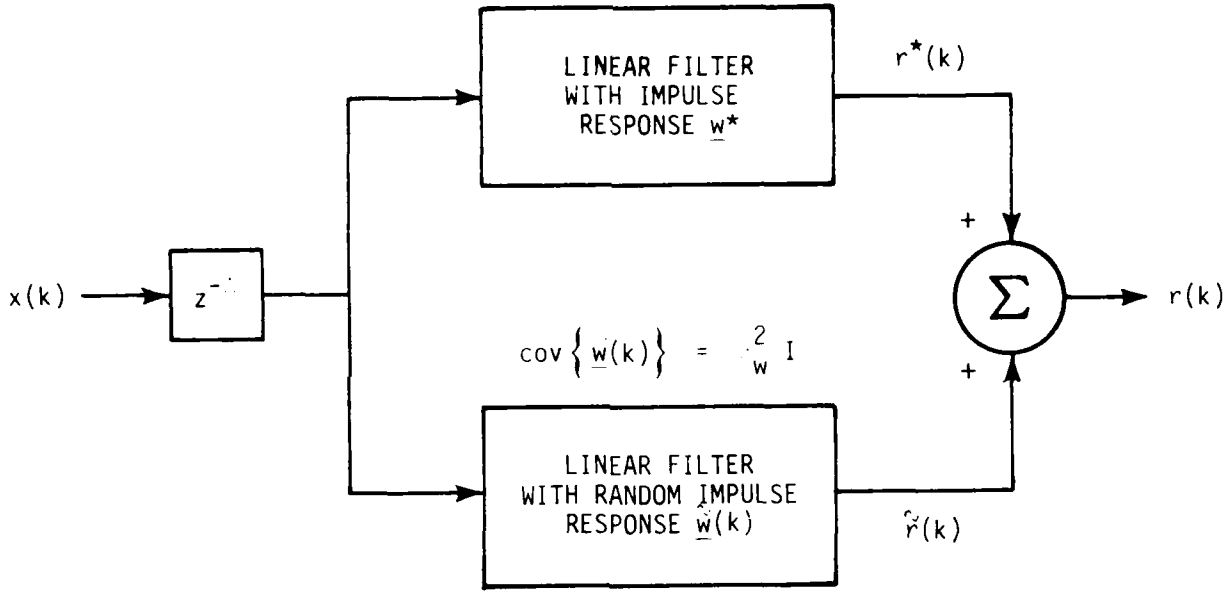

Figure 2. Equivalent model for steady-state ALE for narrowband signals in white noise.

optimum Wiener Δ-step predictor weight vector, and $\tilde{\underline{w}}(k)$ is a very slowly fluctuating vector random process with a mean value of zero. Under the assumptions of relatively slow adaptation, low input SNR, and white Gaussian input noise, the weight vector "misadjustment" $\tilde{\underline{w}}(k)$ is assumed to be independent of the current data in the filter. Thus, the steady-state weight vector may be treated as a Gaussian random variable $\underline{w}$ with mean $\underline{w}^*$ and covariance $\sigma_w^2 I$, where $\sigma_w^2 = \mu\xi_{min}$ and ξ_{min} is the minimum mean squared error associated with Wiener filtering of the input [1].

For the equivalent model of the steady-state ALE illustrated in Figure 2, the output $r(k)$ is a superposition of the Wiener filter (WF) and misadjustment filter (MF) outputs, i.e.,

$$r(k) = r^*(k) + \tilde{r}(k). \tag{4}$$

For an input $x(k)$ comprised of a signal and noise components, $r(k)$ is thus a sum of four terms--WF signal, WF noise, MF signal, and MF noise. The output SNR can be calculated as the power in the WF signal component divided by the total power contributed by the other three terms. The gain of the ALE can then be found by dividing the output SNR by the input SNR.

In the sections that follow, a description of the procedure used to derive the impulse response of an ideal Wiener filter, $\underline{w}^*$, will be given in Section 3.1. These results will then be applied to obtain $\underline{w}^*$ and the Wiener filter transfer function $H^*(\omega)$ for the special case of a narrowband input signal in additive WGN in Section 3.2. The output SNR gain of the ALE will be defined and computed in Section 4 as a function of input and adaptive filter parameters.

3.0 DETERMINATION OF THE MEAN LPF COEFFICIENTS

3.1 Generalized Inputs

Referring back to Figure 1, the LPF coefficients, $w^*(k)$, which minimize the power in the error sequence $\varepsilon(k)$, satisfy the discrete form of the Wiener-Hopf equation,

$$\sum_{k=0}^{L-1} \phi_{xx}(\ell-k)\, w^*(k) \;=\; \phi_{xx}(\ell+\Delta), \qquad \ell = 0,1,\ldots,L-1. \tag{5}$$

The series $\phi_{xx}(\ell) = E[\overline{x(k)}\, x(k+\ell)]$, where the overbar denotes complex conjugation, is the autocorrelation of the stationary input $x(k)$. The set of L linear equations described by Equation (5) can be solved by elementary methods if the z-transform of $\phi_{xx}(\ell)$,

$$S_{xx}(z) \;\equiv\; \sum_{\ell=-\infty}^{\infty} \phi_{xx}(\ell)\, z^{-\ell},$$

is a rational function of z [35]. The assumption of stationarity means that $S_{xx}(z) = \overline{S_{xx}}(1/\bar{z})$ for all complex values of z, and therefore

$$S_{xx}(z) = H(z)\bar{H}(1/\bar{z}) = K\, \frac{\prod_{q=1}^{Q} \left(z-e^{-\beta_q+j\psi_q}\right)\left(z^{-1}-e^{-\beta_q-j\psi_q}\right)}{\prod_{p=1}^{P} \left(z-e^{-\alpha_p+j\omega_p}\right)\left(z^{-1}-e^{-\alpha_p-j\omega_p}\right)} \tag{6}$$

where K, α_p, β_q are positive real constants, and ω_p, ψ_q lie in the closed interval $[-\pi,\pi]$. Thus, $S_{xx}(z)$ is characterized by P pairs of poles at $z = \exp(\pm\alpha_p+j\omega_p)$ and Q pairs of zeroes at $z = \exp(\pm\beta_q+j\psi_q)$. The expansion in Equation (6) with $z = \exp(j\omega)$ represents the power spectrum of a complex process. For a real process, any complex poles and zeroes of $S_{xx}(z)$ will appear in quadruplet sets because of the presence of conjugate pairs at $z = \exp(\pm\alpha_p-j\omega_p)$ and $z = \exp(\pm\beta_q-j\psi_q)$.

The general form for the solution to Equation (5) for stationary inputs with rational power spectra such as that described by Equation (6) is derived in [35]. In the case where number of zeroes of $S_{xx}(z)$ does not exceed the number of poles ($Q \leq P$), the LPF coefficients can be expressed as

$$w^*(k) = \sum_{q=1}^{Q} \left\{ B_q^+ e^{-\beta_q k + j\psi_q} + B_q^- e^{-\beta_q (L-1-k) + j\psi_q} \right\} + \sum_{r=1}^{P-Q} \left\{ C_r^+ \delta(k-r+1) + C_r^- \delta(k+r-L) \right\}, k = 0,1,\ldots,L-1, \quad (7)$$

where $\delta(k)$ is the Kronecker delta function. Note that, in general, $w^*(k)$ consists of sums of damped exponentials as well as impulses. The complex exponentials $\exp(\pm\beta_q + j\psi_q)$ are the zeroes of $S_{xx}(z)$, and the amplitudes of the terms decaying from the beginning (k=0) and end (k = L-1) of the filter are symbolized by the constants B_q^+ and B_q^-, respectively. Similarly, C_r^+ and C_r^- represent the amplitudes of impulses that appear at k = r-1 and k = L-r when P > Q. The constants with a "+" superscript can be thought of as forward terms, while those having a "-" are associated with reflection terms which occur because of the finite filter length L [1]. The values of $B_q^{\pm}$ and $C_r^{\pm}$ can be determined by solving the set of 2P coupled equations obtained from substituting the expression for $w^*(k)$ given in Equation (7) into Equation (5) provided that $\phi_{xx}(\ell)$ is known explicitly [35].

3.2 Narrowband Signals Embedded in WGN

The primary difficulty in applying Equation (7) to obtain the mean LPF response is that it requires a pole-zero model for the LPF input autocorrelation in the form defined by Equation (6) [1]. For mutually uncorrelated narrowband processes embedded in additive broadband noise,

$$\phi_{xx}(\ell) = \phi_{ss}(\ell) + \phi_{nn}(\ell) \tag{8}$$

and

$$S_{xx}(z) = S_{ss}(z) + S_{nn}(z), \tag{9}$$

where the signal transform $S_{ss}(z)$ and the noise transform $S_{nn}(z)$ are known rational functions of the type described by Equation (6).

Although the poles of $S_{xx}(z)$ are simply the sum of those of $S_{ss}(z)$ plus any contributed by $S_{nn}(z)$, its zeroes do not have a simple analytic form in the general case. However, as explained in [35], approximate expressions for the values β_q, ψ_q of $S_{xx}(z)$ can be derived if $S_{ss}(z)$ is comprised of pole pairs lying sufficiently close to the unit circle that their contributions to the total power spectrum do not overlap appreciably. Under these conditions of widely-spaced narrowband signal processes, the background noise spectral density can be approximated by evaluating $S_{xx}(e^{j\omega})$ at frequencies away from the vicinity of the poles of $S_{ss}(z)$. The transform of the total input is then expressed as the product

$$S_{xx}(z) \approx S_{nn}(z)\, R(z), \tag{10}$$

where $R(z)$ is a rational function of z characterized by the poles of $S_{ss}(z)$ and an equal number of zeroes located on the same radial lines [35]. Equation (10) implies that when broadband noise having P_n pairs of poles and Q_n pairs of zeroes is added to narrowband signals having P_s pole pairs, the total input process may be approximated by an

autoregressive, moving-average (ARMA) model with $2(P_s+P_n)$ poles and $2(P_s+Q_n)$ zeroes.

The utility of the general approach outlined above is now demonstrated by consideration of a simple example. Assume that the input autocorrelation is real and consists of a finite bandwidth signal embedded in uncorrelated noise, i.e.,

$$\phi_{xx}(\ell) = \sigma^2 e^{-\alpha|\ell|} \cos \omega_o \ell + \nu^2 \delta(\ell), \tag{11}$$

where σ^2, α, and ω_o represent the power, 3 dB half bandwidth, and center frequency of the signal and ν^2 is the power of the noise.* In this case, the z-transform of the narrowband signal term,

$$S_{ss}(z) = \frac{\sigma^2(1-e^{-2\alpha})}{2} \left[\frac{1}{(z-e^{-\alpha+j\omega_0})(z^{-1}-e^{-\alpha-j\omega_0})} + \frac{1}{(z-e^{-\alpha-j\omega_0})(z^{-1}-e^{-\alpha+j\omega_0})} \right]$$

has four poles at $\exp(\pm\alpha\pm j\omega_0)$. Noting that $S_{nn}(z) = \nu^2$ has neither poles nor zeroes and using the approximation given in Eq. (10) valid for $\alpha << 1$,

$$S_{xx}(z) = \nu^2 \frac{(z-e^{-\beta+j\omega_0})(z-e^{\beta+j\omega_0})(z-e^{-\beta-j\omega_0})(z-e^{\beta-j\omega_0})}{(z-e^{-\alpha+j\omega_0})(z-e^{\alpha+j\omega_0})(z-e^{-\alpha-j\omega_0})(z-e^{\alpha-j\omega_0})}. \tag{12}$$

Thus, the z-transform of the total input has four zeroes located at different distances away from the unit circle, but on the same radial lines as the signal poles. In terms of these zeroes at $\exp(\pm\beta\pm j\omega_0)$, the LPF coefficients for the real input autocorrelation designated in Equation (11) are written in a manner analogous to the general form of Equation (7), i.e.,

---

*Note that because $\phi_{xx}(0) = \sigma^2+\nu^2$ does not depend upon α, it is the total energy in the input spectrum that is held constant in this model.

$$w^*(k) = \left[B^+ e^{-\beta k} + B^- e^{-\beta(L-1-k)}\right] \cos \omega_0(k+\tfrac{1}{2}). \qquad (13)$$

The constants β, B^+, and B^- are determined by substituting Equations (11) and (13) into (5). Assuming the prediction distance $\Delta > 0$ and neglecting the summation over non-stationary cosine terms ($L \gg 1$), the resultant equation contains exponential terms of the form $e^{-\beta\ell}$, $e^{-\beta(L-1-\ell)}$, $e^{-\alpha\ell}$ and $e^{-\alpha(L-1-\ell)}$. Grouping terms of either of the first two of these types specifies the relationship between the zero and pole locations in (12) to be

$$\cosh \beta = \cosh \alpha + \frac{SNR}{2} \sinh \alpha, \qquad (14)$$

where α is the input signal bandwidth and $SNR \triangleq \sigma^2/\nu^2$. As derived in [35] for a more general case, the above equation implies that for poles and zeroes close to the unit circle,

$$\beta \approx \sqrt{\alpha(\alpha + SNR)}, \qquad \alpha, \beta << 1. \qquad (15)$$

This dependence of filter bandwidth on signal bandwidth and broadband input SNR is illustrated graphically in Figure 3. Note that the plot of β vs. SNR for each different value of α can be characterized by two linear asymptotes. To the left of the breakpoint at SNR = α, the curves become horizontal, indicating that $\beta \to \alpha$ in the limit of noise only input. To the right of the breakpoint, the filter bandwidth may be approximated by the line $\beta = \sqrt{\alpha SNR}$ in the logarithmic plot.

Determined in a similar manner by equating coefficients in $e^{-\alpha\ell}$ and $e^{-\alpha(L-1-\ell)}$, the forward and reflection amplitudes are:

$$B^+ = \frac{2e^{-\alpha\Delta}(\beta-\alpha)(\beta+\alpha)^2}{(\beta+\alpha)^2 - e^{-2\beta L}(\beta-\alpha)^2} \qquad (16a)$$

and

$$B^- = \frac{2e^{-\alpha\Delta}(\beta+\alpha)(\beta-\alpha)^2 e^{-\beta(L+1)}}{(\beta+\alpha)^2 - e^{-2\beta L}(\beta-\alpha)^2}, \qquad \alpha, \beta << 1. \qquad (16b)$$

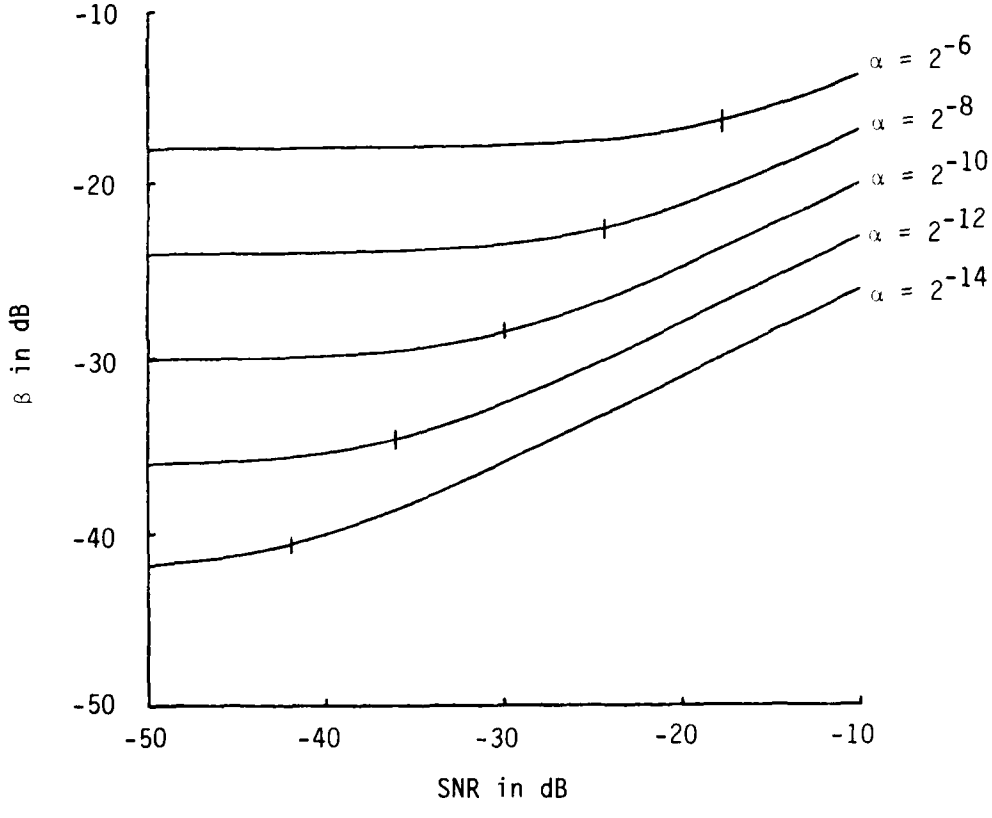

Figure 3. Filter bandwidth vs. input SNR for several values of signal bandwidth. The small vertical bar on each curve indicates the breakpoint where SNR = α.

Equations (13) through (16) provide a complete description of the solution to the Wiener-Hopf equation for an input consisting of a real narrowband process in additive uncorrelated noise.

The frequency response of the LPF is now determined as the sum of the transforms of the forward and reflection components of $w_k^*(L,\Delta)$, i.e.,

$$H^*(\omega) = \sum_{k=0}^{L-1} B^+ e^{-\beta k} \cos \omega_0(k+\Delta) e^{-j\omega k} + \sum_{k=0}^{L-1} B^- e^{-\beta(L-1-k)} \cos \omega_0(k+\Delta) e^{-j\omega k}.$$

Performing the summations and taking the magnitude-squared assuming no spectral overlap of positive and negative frequencies,

$$|H^*(\omega)|^2 = \frac{e^{-\beta(L-1)}}{2} \left\{ \frac{B^{+2} + B^{-2}}{2} \frac{\cosh \beta L - \cos xL}{\cosh \beta - \cos x} + B^+B^- \frac{(\cosh\beta \cos x - 1)(\cosh\beta L \cos xL - 1) - \sinh\beta \sin x \sinh\beta L \sin xL}{(\cosh \beta - \cos x)^2} \right\}, \tag{17}$$

where the variable x is used to denote the frequency difference $\omega - \omega_0$.

The frequency response described by Equation (17) is plotted in Figure 4 for fixed μ, Δ, L, and α. The tendency of the Wiener filter to turn itself off in the absence of correlated inputs is evidenced by the downward shift in $|H^*(\omega)|^2$ for decreasing values of input SNR. Note also that the vertical bars marking the 3 dB bandwidth of the filter appear at frequencies approximately equal to $\omega_0 \pm \alpha$ for SNR $< \alpha$, but they spread farther apart for higher SNR. This broadening of filter bandwidth, already evident from the plots of β that appeared in Figure 3, may be interpreted as follows: In the low SNR case, the frequency response of the LPF must be narrow in order to suppress the rather large amount of noise power present in the vicinity of the signal. As the relative strength of the signal increases, however, the transform of the filter can afford to widen in order to respond to the signal components at $\omega \neq \omega_0$, without passing significantly more noise power.

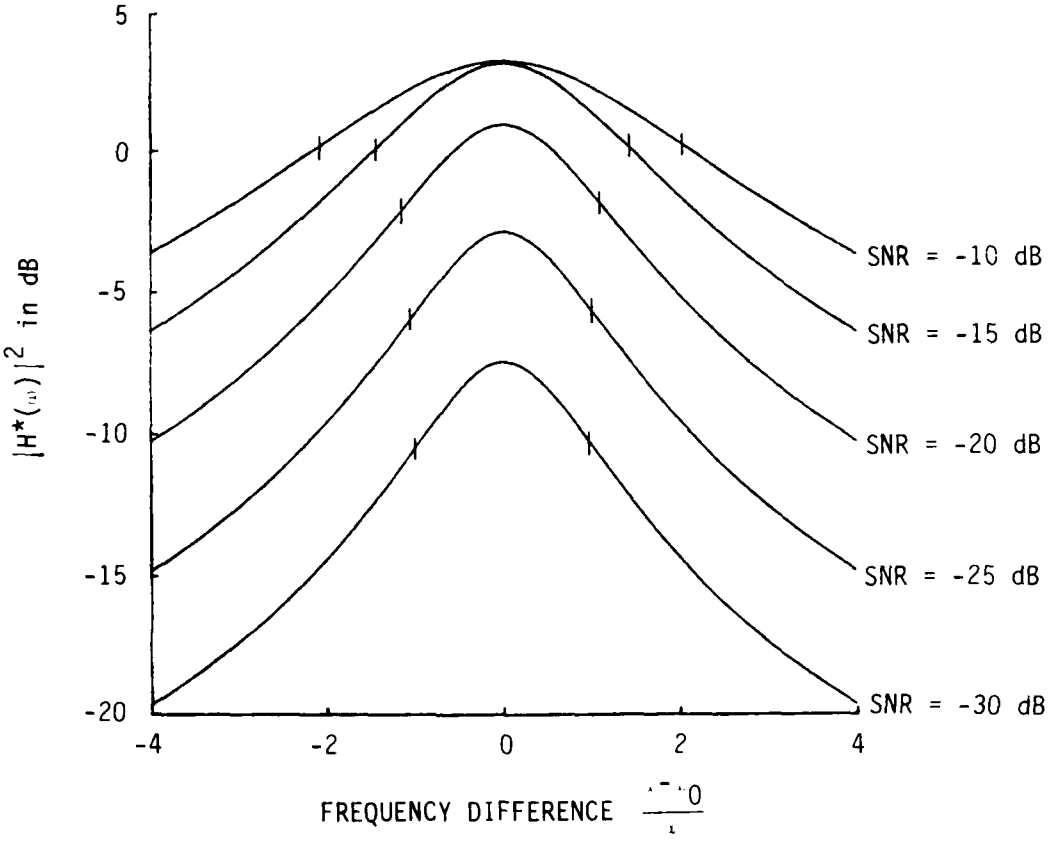

Figure 4. Frequency response of Wiener filter for several values of SNR where $\mu = 2^{-13}$, $\Delta = 1$, $\alpha = 2^{-5} \cong -15$ dB, $L = 16/\alpha = 512$. Small vertical bars mark $\omega = \omega_0 \pm \beta$, the 3 dB filter bandwidth.

Unlike the filter bandwidth β, the amplitude coefficients B^+ and B^- appearing in Equation (13) depend upon the filter parameters Δ and L as well as input SNR. First, observe that the values of both the forward and reflection amplitudes given in Equation (16) are proportional to $\exp(-\alpha\Delta)$. This implies that for a fixed value of $\alpha > 0$, the magnitude of $w^*(k)$ diminishes as the input signal suffers greater decorrelation for increasing values of bulk delay. Second, note that the contribution of the reflection term relative to that of the forward term is dependent upon the filter length, i.e.,

$$\frac{B^-}{B^+} \approx e^{-\beta(L+1)} \frac{(\beta-\alpha)}{(\beta+\alpha)}$$

for $\alpha, \beta << 1$. Thus, for $L >> 1/\beta$, the relative value of the reflection term approaches zero, and $w_k^*(L,\Delta)$ is comprised solely of a damped sinusoid decaying from the beginning of the filter, in agreement with the infinite length Wiener filter discussed in [39].

There is another limiting case of interest. Under conditions where the filter length is sufficiently short relative to the signal bandwidth that $\beta L \to 0$ for all SNR, the input resembles a single sinusoid in white noise. Consideration of this case is important both as a check on the results presented above and as a means of comparing the behavior of the LPF for inputs of finite versus infinitesimal bandwidths. Assuming that $\exp(-\beta k)$ is approximately unity for all $0 \leq k < L$, the Wiener coefficients given in Equation (13) simplify to

$$w^*(k) = (B^+ + B^-) \cos \omega_0(k+\Delta), \qquad \beta L << 1,$$

a constant times the phase-compensated input signal. In the limit as $\beta L \to 0$, both B^+ and B^- computed in (16) approach the same value. In terms of the definition used in previous studies,

$$a^* \triangleq \frac{L\ SNR/2}{1 + L\ SNR/2},$$

the forward and reflection amplitudes are $B^+ = B^- = \exp(-\alpha\Delta)a^*/L$. Therefore, Equation (13) gives

$$w^*(k) = \frac{2a^*}{L} e^{-\alpha\Delta} \cos \omega_0(k+\Delta), \qquad \beta L << 1,$$

which agrees with previous results provided the delay Δ does not decorrelate the signal. Thus for $\Delta << \alpha^{-1}$, the performance of the LPF of length $L << (\alpha^2 + \alpha SNR)^{-\frac{1}{2}}$ for a finite bandwidth signal in white noise approaches that achieved for a pure sinusoid embedded in the same broadband background.

4.0 SECOND-ORDER OUTPUT STATISTICS FOR NARROWBAND SIGNALS IN WGN

Recalling the weight vector model described in Section 2, the ALE output for narrowband inputs in WGN is comprised of four additive components: (1) Wiener-filtered (WF) signal; (2) WF noise; (3) misadjustment filtered (MF) signal; and(4) MF noise. The general behavior of their second-order statistics is typified by the power spectral densities displayed in Figure 5. Note from Figure 5a that the WF signal spectrum, the result of passing a narrowband input through a narrowband filter, exhibits sharp attenuation for frequencies away from the signal center frequency. The two WF terms match at $\cdot = \cdot_0$ because $S_{ss}(\cdot_0)/S_{nn}(\cdot_0) = SNR/$ is approximately unity in this particular example. For the same reason, the power spectral densities of the MF terms displayed in Figure 5b are also equal to one another at the center frequency, but at a level of more than 20 dB lower than those of the WF terms.

Broadband gain, dependent upon the total power over the entire frequency spectrum, can be calculated directly from the input autocorrelation given in (11) and the convergent ALE weight vector described in (13). Representing the autocorrelations of the four mutually uncorrelated components of r(k) as $\phi_s^*(\ell)$, $\phi_n^*(\ell)$, $\tilde{\phi}_s(\ell)$, and $\tilde{\phi}_n(\ell)$, the output SNR is

$$SNR_o = \frac{\phi_s^*(0)}{\phi_n^*(0) + \tilde{\phi}_s(0) + \tilde{\phi}_n(0)} . \qquad (18)$$

The sum of the output autocorrelations for the two misadjustment terms is

$$\tilde{\phi}(0) = \tilde{\phi}_s(0) + \tilde{\phi}_n(0) = \mu\zeta_{min} L(\sigma^2 + \nu^2) \qquad (19)$$

where ζ_{min}, the minimum mean-squared error associated with Wiener filtering of the input, is approximately equal to ν^2 for large values of L [3]. Assuming a sufficiently long filter length, the WF noise component is

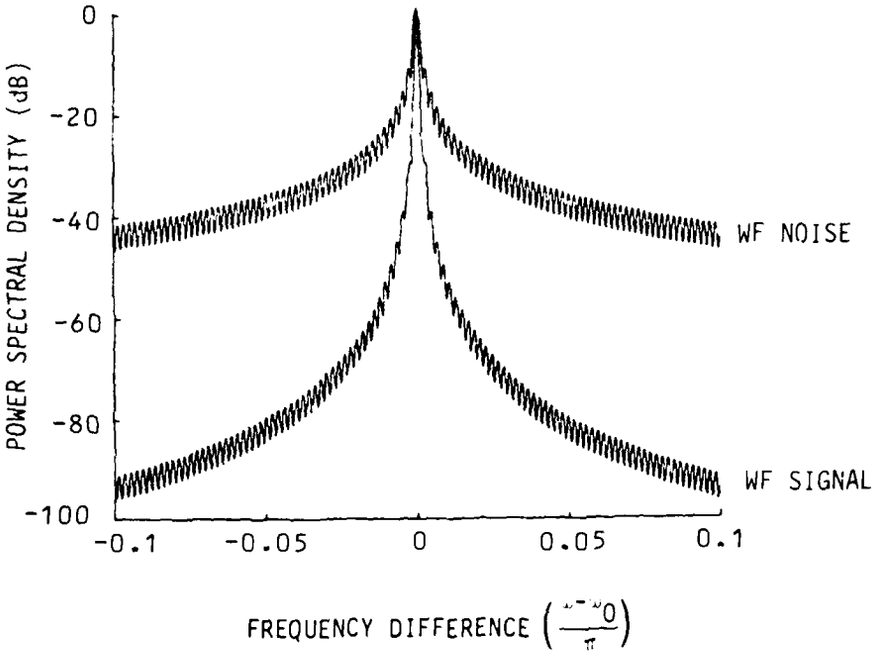

a. WF signal and noise terms.

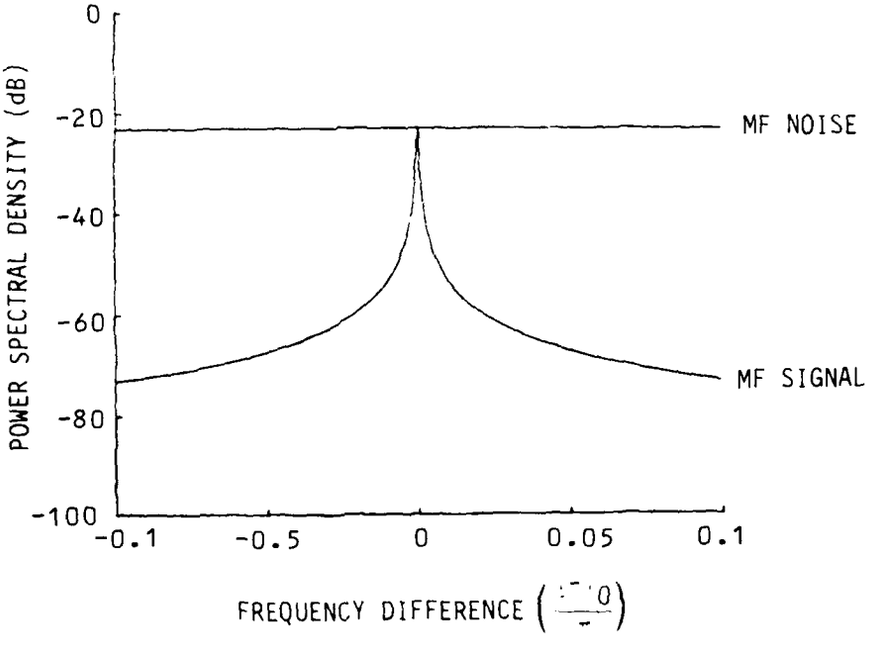

b. MF signal and noise terms.

Figure 5. Power spectral densities of the four ALE output components for the parameters $\mu = 2^{-13}$, $\Lambda = 1$, $L = 1024$, $\alpha = 1/L$, $SNR_{in} = -30$ dB.

$$\phi_n^*(0) = \sum_{k=1}^{L-1} \sum_{\ell=0}^{L-1} w_k^* w_\ell^* \nu^2 \delta(k-\ell) \tag{20}$$

$$= \nu^2 e^{-\beta L} \left\{ \frac{(B^+)^2 + (B^-)^2}{2\beta} \sinh \beta L + B^+ B^- L \right\}, \quad \alpha, \beta \ll 1$$
$$L \gg 1.$$

Using the same assumptions, the WF signal term is evaluated:

$$\phi_s^*(0) = \sum_{k=0}^{L-1} \sum_{\ell=0}^{L-1} w_k^* w_\ell^* \sigma^2 e^{-\alpha|k-\ell|} \cos(k-\ell)\omega_0$$

$$= \frac{\sigma^2 e^{-\beta L}}{\beta^2 - \alpha^2} \left\{ \frac{(B^+)^2 + (B^-)^2}{2} \left[\cosh \beta L - \frac{\alpha}{\beta} \sinh \beta L - e^{-\alpha L} \right] \right. \tag{21}$$

$$\left. + B^+ B^- \left[\frac{e^{-\alpha L}[(\beta^2+\alpha^2)\cosh \beta L + 2\alpha\beta \sinh \beta L] - (\beta^2+\alpha^2)}{\beta^2 - \alpha^2} - \alpha L \right] \right\}.$$

Broadband ALE gain is determined by the ratio of (21) divided by the sum of (19) and (20) to input $SNR_i = \sigma^2/\nu^2$. The effects of input signal variables and filter parameters are illustrated in Figures 6 through 9. In all cases, the total input power is held constant ($\sigma^2 + \nu^2 = 0.04$), and the ALE feedback parameter is also fixed ($\mu = 2^{-13}$). As a demonstration of the result of increasing signal bandwidth, broadband gain is plotted as a function of input SNR in Figure 6 for $\omega_0 = 1$, $L = 1024$, and α varying from zero to 16 times the ALE resolution ($1/L$). Note from the shift downward and to the right that gain decreases for increasing α and the performance is most severely degraded at low values of input SNR.

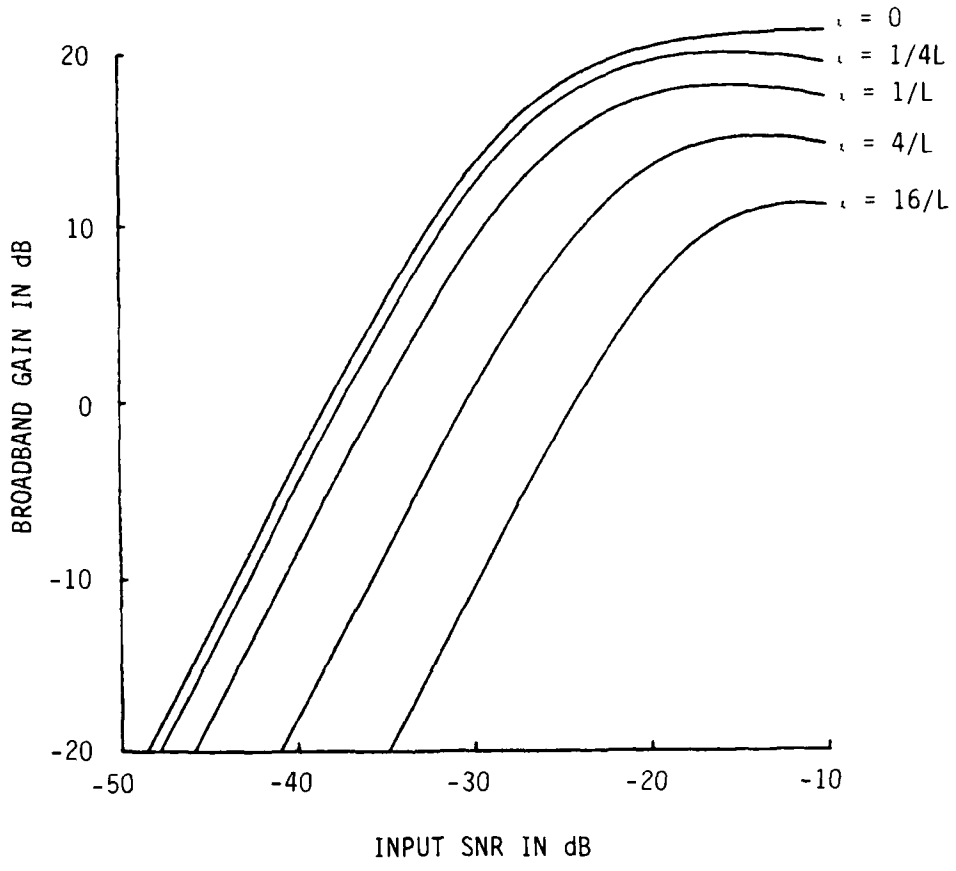

Figure 6. Broadband ALE gain vs. input SNR for several values of signal bandwidth (α = 0 represents sinusoidal limit). Filter parameters are $\mu = 2^{-13}$, Δ = 1, and L = 1024.

The effect of filter parameters L and Δ is shown in Figure 7. In 7a, gain vs. SNR is plotted for signal bandwidth and filter length fixed, and bulk delay varying from unity to 3 times L. As expected, ALE gain decreases exponentially as a function of the product $\alpha\Delta$ due to increasing signal decorrelation. The dependence of gain upon filter length is more complicated, however. Note from the crossing curves in Figure 7b that for fixed α and Δ, the value of L yielding the maximum gain is equal to or less than the inverse signal bandwidth, depending upon the input SNR.

In order to demonstrate the relationship between the optimum filter length and the input signal variables, broadband gain is plotted as a function of L for several values of α and SNR in Figure 8. From 8a, it is obvious that for low SNR, the peak in the gain curves for each value of α coincides with the small vertical bar which marks the point where $L = 1/\alpha$. The same is true only for the two lower curves in Figure 8b, where $\alpha > \text{SNR} \cong 2^{-10}$; the optimum L for $\alpha \leq 2^{-10}$ is left of the $1/\alpha$ mark. The family of curves in 8c shows that for SNR $>>$ α, gain is less sensitive to the choice of L.

As further clarification of ALE gain performance as a function of filter length, component terms are plotted in Figure 9 for moderate and high SNR conditions. The three curves displayed in each case represent WF signal ($\phi_s^*(0)$), WF noise ($\phi_n^*(0)$) and MF signal plus noise ($\tilde{\phi}(0)$). Looking first at 9a, note that $\phi_n^*(0) << \tilde{\phi}(0)$ for all L and thus broadband noise at the output is dominated by the misadjustment terms regardless of ALE filter length. The $\phi_s^*(0)$ numerator component rises quite rapidly with increasing L and then saturates at about $L = 1/\beta$, the point marked by the small vertical bar. This explains why the ALE gain curve ($\alpha = 2^{-10}$) appearing in Figure 8b exhibited a maximum for that value of L. The component terms displayed in 9b illustrate that for high SNR, the behavior is not so simple. Although the $\phi_s^*(0)$ shows the same saturation behavior in the vicinity of $L = 1/\beta$, the output noise is not dominated by the linearly increasing misadjustment terms except for very long filter lengths where

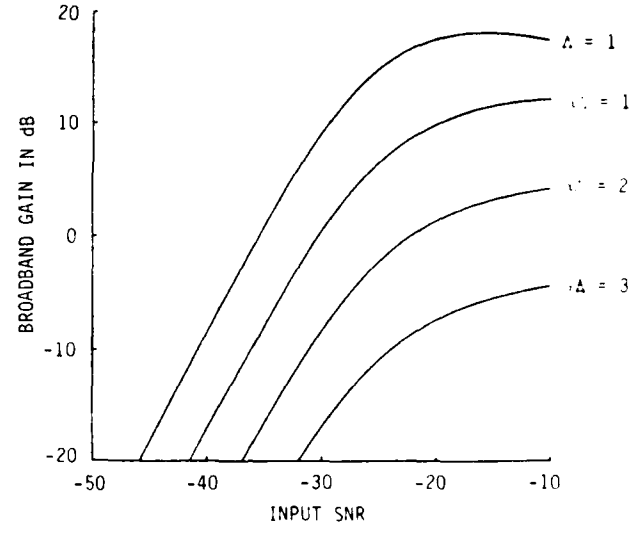

a. Different values of bulk delay Δ (L = 1/4).

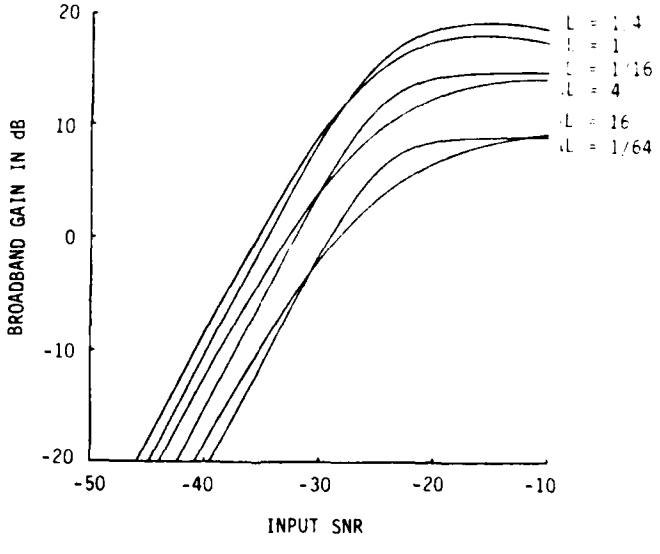

b. Different values of filter length L (Δ = 1).

Figure 7. The effect of filter parameters on broadband gain curves ($\mu = 2^{-13}$, $\alpha = 2^{-10}$).

a. SNR_{in} = -50 dB.

b. SNR_{in} = -30 dB.

c. SNR_{in} = -10 dB.

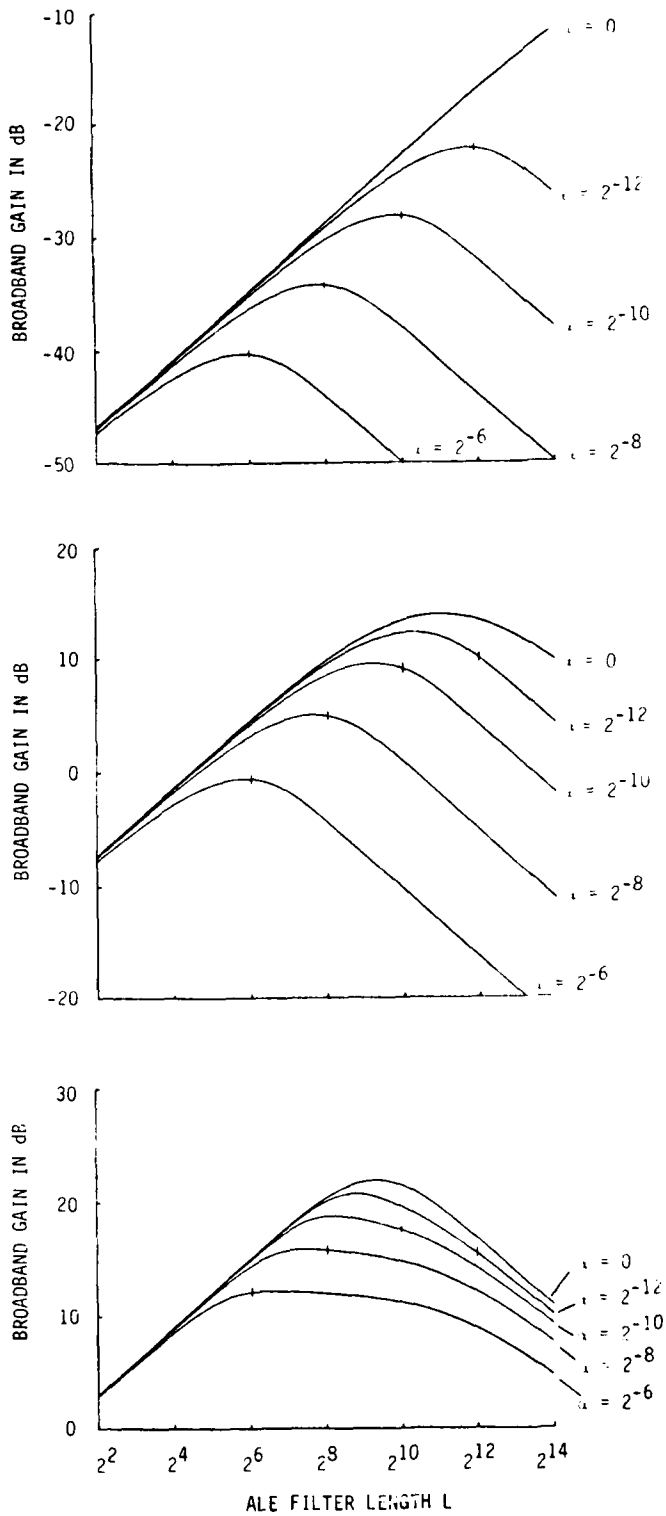

Figure 8. Optimal filter length determination as a function of signal bandwidth and SNR. ($\mu = 2^{-13}$, $\Delta = 1$, small vertical bars indicate $L = 1/\alpha$ for each curve).

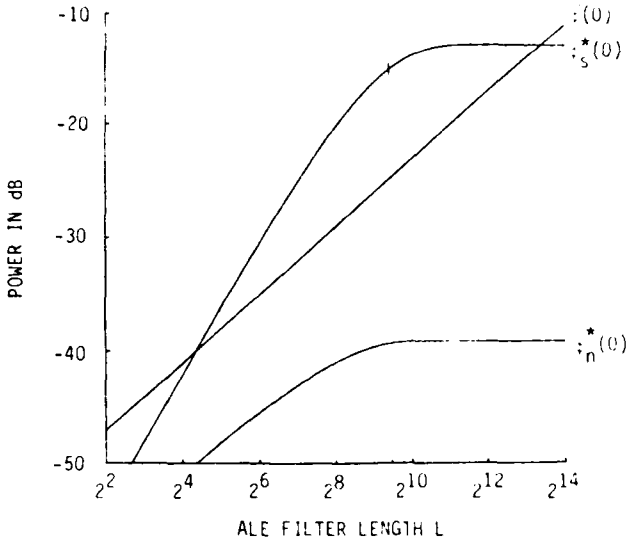

a. SNR_{in} = -30 dB.

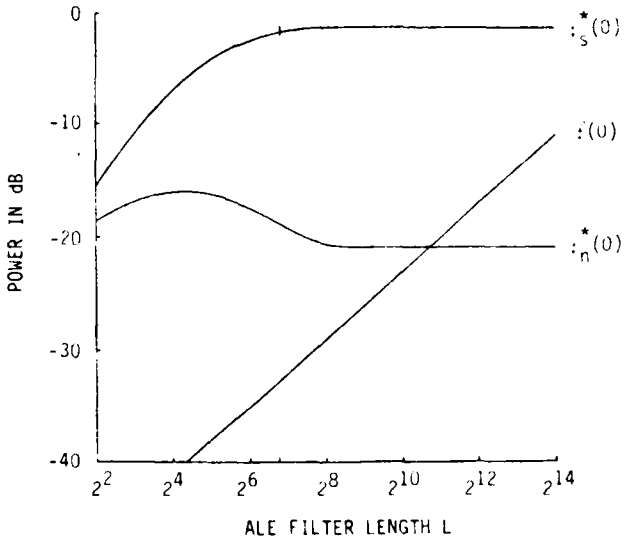

b. SNR_{in} = -10 dB.

Figure 9. Component terms for broadband gain for $\mu = 2^{-13}$, $\Lambda = 1$, $\alpha = 1/1024$. Small vertical bars on $\phi_s^*(0)$ curve mark filter length $L = 1/\beta$.

$\beta L \gg 1$ and there are a significant number of unused adaptive weights. The flattened gain curve in Figure 8c reflects the behavior of these components.

5.0 CONCLUSIONS

The steady-state behavior of the adaptive line enhancer (ALE) has been analyzed in this paper for stationary inputs consisting of narrowband signals embedded in additive broadband noise. The narrowband signals were modeled as the output of a bandpass filter of finite bandwidth α, centered at a specified frequency ω_0. Assuming non-overlapping signal spectra ($\alpha << 1$ and $0 << \omega_0 << \pi$), analytic expressions for the ALE weights and output were derived as functions of input and adaptive filter parameters. The steady-state ALE has been decomposed into two components: a deterministic, time-invariant Wiener prediction filter (WF) and a slowly-varying, random misadjustment filter (MF). The relative contributions of these two filters were discussed, and it was shown that the MF components can be neglected only in certain cases of high input signal-to-noise ratio (SNR).

An appropriate pole-zero model was defined which allowed the WF solution to be determined for an arbitrary prediction distance (Δ) and number of adaptive weights (L). It was demonstrated that the WF takes the form of a bandpass filter centered at frequency ω_0. The bandwidth (β) of the Wiener filter was shown to be a function of input SNR and signal bandwidth. It was emphasized that the value of β exceeds that of α, except for very low input SNR conditions where the filter and signal bandwidths match. The general expressions for the WF impulse response and transfer function herein derived have been simplified for two limiting cases--one in which the length of the transverse adaptive filter is sufficiently long that $\beta L >> 1$, and the other in which $\beta L << 1$ for the input signal bandwidth and SNR of interest. The results for this latter limit were shown to agree with those previously derived for sinusoids in WGN [26].

The output of the steady-state ALE was modeled as the sum of four independent components--one considered signal and the other three regarded as noise. The output signal component corresponds to

the narrowband input filtered through the WF, while the output noise consists of WF filtered noise as well as MF filtered signal and noise terms. Second-order statistical properties of these four output components were derived, and an expression was given for the broadband ALE gain, the ratio of output SNR to that of the input. For fixed ALE parameters, the gain of the adaptive filter was shown to decrease with increasing input signal bandwidth and/or diminishing input SNR. In the limit as α approaches zero, the gain expressions herein derived reduce to those previously reported for adaptive enhancement of sinusoids in WGN [26].

The determination of optimal ALE length and bulk delay parameters for given input bandwidth and SNR has also been discsussed in this paper. For the narrowband signal model used here, broadband ALE gain decreases approximately exponentially as a function of increasing values of the product $\alpha\Delta$. Because of this effect which results from decorrelation of a finite bandwidth signal, the ALE bulk delay should not exceed $1/\alpha$ when the input noise is uncorrelated. The choice of optimal filter length is more complicated and depends upon input SNR as well as signal bandwidth. Under low SNR conditions where the MF terms dominate the ALE output noise, $L_{opt} \approx 1/\alpha$. For higher SNR where the WF noise component contributes significantly, maximum gain is typically achieved for a filter length shorter than the inverse signal bandwidth. The major effect is that attempting to over-resolve narrowband signals by increasing L eventually degrades ALE gain because of larger misadjustment noise at the output. Although these results relate specifically to applications in which the LMS adaption is used to estimate WF coefficients, they emphasize the importance of including the effects of algorithm misadjustment noise in the performance analysis of real-time adaptive processors.

Because of the inclusion of a finite bandwidth parameter, the approach presented in this paper has relevance to more realistic ALE scenarios than the previously reported studies for sinusoidal input signals embedded in broadband noise. In addition, the WF analysis developed here may be applied to a larger class of LPF problems such as systems identification and speech enhancement. In applications where LPF coefficients are used to estimate signal parameters, our analysis indicates that distortions in both amplitude and bandwidth will occur for finite bandwidth signals. The results presented in this paper may provide a method for modeling this distortion for the transversal linear prediction filter.

REFERENCES

1. B. Widrow et al., "Adaptive Noise Cancelling: Principles and Applications," Proc. IEEE, 63, pp. 1692-1716, Dec. 1975.

2. M. Sondhi and D. Berkley, "Silencing Echoes on the Telephone Network," Proc. of the IEEE, 68, pp. 948-963, Aug. 1980.

3. N. Verhoeckx, H. van den Elzen, F. Snijders, and P. Gerwen, "Digital Echo Cancellation for Baseband Data Transmission," IEEE Trans. on Acoustics, Speech, and Sig. Proc., ASSP-27, pp. 768-781, Dec. 1979.

4. A. Gersho, "Adaptive Equalization of Highly Dispersive Channels for Data Transmission," Bell Systems Tech. J., 48, pp. 55-70, Jan. 1969.

5. E. Satorius and S. T. Alexander, "Channel Equalization using Adaptive Lattice Algorithms," IEEE Trans. on Communications, COM-27, pp. 899-905, June 1979.

6. E. Satorius and J. Pack, "Application of Least Squares Lattice Algorithms to Adaptive Equalization," IEEE Trans. on Comm., COM-29, pp. 136-142, Feb. 1981.

7. L. J. Griffiths, F. R. Smolka, and L. D. Trembly, "Adaptive Deconvolution: A New Technique for Processing Seismic Data," Geophysics, 42, pp. 742-759, June 1977.

8. L. J. Griffiths, "Rapid Measurement of Digital Instantaneous Frequency," IEEE Trans. on Acoustics, Speech, and Sig. Proc., ASSP-23, pp. 209-222, April 1975.

9. R. Keeler and L. J. Griffiths, "Acoustic Doppler Extraction by Adaptive Linear Prediction," J. Acous. Soc. Amer., 61, pp. 1218-1227, May 1977.

10. N. Bershad, P. Feintuch, F. Reed, and B. Fisher, "Tracking Characteristics of the LMS Adaptive Line Enhancer--Response to a Linear Chirp Signal in Noise," IEEE Trans. on Acoustics, Speech, and Sig. Proc., ASSP-28, pp. 504-517, Oct. 1980.

11. S. Boll and D. Pulsipher, "Suppression of Acoustic Noise in Speech Using Two Microphone Adaptive Noise Cancellation," IEEE Trans. on Acoustics, Speech, and Sig. Proc., ASSP-28, pp. 752-753, Dec. 1980.

12. M. Sambur, "Adaptive Noise Cancelling for Speech Signals," IEEE Trans. on Acoustics, Speech, and Sig. Proc., ASSP-26, pp. 419-423, Oct. 1978.

13. D. Morgan and S. Craig, "Real Time Linear Prediction Using the Least Mean Square Gradient Algorithm," IEEE Trans. on Acoustics, Speech, and Sig. Proc., ASSP-24, pp. 494-507, Dec. 1976.

14. A. Kikuchi, S. Omatu and T. Soeda, "Applications of Adaptive Digital Filtering to the Data Processing for the Environmental System," IEEE Trans. on Acoustics, Speech, and Sig. Proc., ASSP-27, pp. 790-804, Dec. 1979.

15. N. Ahmed, R. Fogler, D. Soldan, G. Elliott, and N. Bourgeois, "On an Intrusion-Detection Approach via Adaptive Prediction," IEEE Trans. on Aerospace and Elec. Sys., AES-15, May 1979.

16. K. Hass, D. Lenhert, and N. Ahmed, "On a Microcomputer Implementation of an Intrusion Detection Algorithm," IEEE Trans. on Acoustics, Speech, and Sig. Proc., ASSP-27, pp. 782-790, Dec. 1979.

17. L. J. Griffiths, "A Simple Adaptive Algorithm for Real-Time Processing in Antenna Arrays," Proc. IEEE, 57, pp. 1696-1704, Oct. 1969.

18. O. L. Frost, III, "An Algorithm for Linearly Constrained Adaptive Array Processing," Proc. IEEE, 60, pp. 926-935, Aug. 1972.

19. R. Compton, "Pointing Accuracy and Dynamic Range in a Steered Beam Antenna Array," IEEE Trans. on Aerospace and Elec. Sys., AES-16, pp. 280-287, May 1980.

20. C. Gibson and S. Haykin, "Learning Characteristics of Adaptive Lattice Filtering Algorithms," IEEE Trans. on Acoustics, Speech, and Sig. Proc., ASSP-28, pp. 681-692, Dec. 1980.

21. R. Compton, "An Adaptive Array in a Spread Spectrum Communication System," Proc. IEEE, 66, pp. 289-298, March 1978.

22. D. Morgan, "Adaptive Multipath Cancellation for Digital Data Communications," IEEE Trans. on Comm., Vol. COM-26, pp. 1380-1390, Sept. 1978.

23. L. Rabiner, R. Crochiere, and J. Allen, "FIR System Modeling and Identification in the Presence of Noise with Band-Limited Inputs," IEEE Trans. on Acoustics, Speech, and Sig. Proc., ASSP-26, pp. 319-333, Aug. 1978.

24. L. Marple, "Efficient Least Squares FIR System Identification," IEEE Trans. on Acoustics, Speech, and Sig. Proc., ASSP-29, pp. 62-73, Feb. 1981.

25. J. Zeidler, E. Satorius, D. Chabries, and H. Wexler, "Adaptive Enhancement of Multiple Sinusoids in Uncorrelated Noise," IEEE Trans. on Acoustics, Speech, and Sig. Proc., ASSP-26, pp. 240-254, June 1978.

26. J. T. Rickard and J. Zeidler, "Second Order Output Statistics of the Adaptive Line Enhancer," IEEE Trans. on Acoustics, Speech, and Sig. Proc., ASSP-27, pp. 31-39, Feb. 1979.

27. J. Treichler, "Transient and Convergent Behavior of the ALE," IEEE Trans. on Acoustics, Speech, and Sig. Proc., ASSP-27, pp. 53-63, Feb. 1979.

28. W. S. Burdic, "Detection of Narrowband Signals Using Time Domain Adaptive Filters," IEEE Trans. on Aerospace and Elec. Sys., AES-14, pp. 578-591, July 1978.

29. J. T. Rickard, J. Zeidler, M. Dentino, and M. Shensa, "A Performance Analysis of Adaptive Line Enhancer-Augmented Spectral Detectors," Joint Special Issue on Adaptive Signal Processing, IEEE Trans. on Acoustics, Speech, and Sig. Proc., ASSP-29, pp. 694-701 and IEEE Trans. on Circuits and Systems, CAS-28, pp. 534-542, June 1981.

30. J. T. Rickard and J. R. Zeidler, 'Coherence Detection Augmented by Adaptive Prefiltering," Proceedings of the 1980 Conference on Information Sciences and Systems, Princeton University, pp. 254-259, March 26-28, 1980.

31. V. Reddy, B. Egardt and T. Kailath, "Optimized Lattice-Form Adaptive Line Enhancer for a Sinusoidal Signal in Broadband Noise," Joint Special Issue on Adaptive Signal Processing, IEEE Trans. on Acoust., Speech, and Sig. Proc., ASSP-29, pp. 702-710, and IEEE Trans. on Circuits and Systems, CAS-28, pp. 543-551, June 1981.

32. B. Egardt, T. Kailath and V. Reddy, "High Resolution Spectral Analysis Using Multistep Adaptive Prediction," submitted to IEEE Transactions on ASSP, October 1980.

33. D. Morgan, "Response of a Delay Constrained Adaptive Linear Prediction Filter to a Sinusoid in White Noise," Proceedings of the 1981 International Conference on Acoustics, Speech and Signal Processing, pp. 271-275, March 28-April 1, 1981.

34. D. L. Duttweiler and Y. S. Chen, "A Single Chip VLSI Echo Canceller," Bell Systems Technical Journal, pp. 149-161, Feb. 1980.

35. E. Satorius, J. Zeidler, and S. Alexander, "Linear Predictive Digital Filtering of Narrowband Processes in Additive Broadband Noise," Naval Ocean Systems Center Technical Report 331, San Diego, CA., November 1978.

36. T. Kailath, "A View of Three Decades of Linear Filtering Theory," IEEE Transactions on Information Theory, Vol. IT-20, pp. 145-181, March 1974.

37. J. Makhoul, "Linear Prediction: A Tutorial Review," Proc. IEEE, 63, pp. 561-580, April 1975.

38. B. Widrow, "Adaptive Filters," in Aspects of Network and Systems Theory, R. Kalman and N. De Claris, eds., New York: Holt, Reinhart and Winston, pp. 563-587, 1971.

39. M. Shensa, "Time Constants and Learning Curves of LMS Adaptive Filters," Naval Ocean Systems Center Technical Report 312, November 1978.

40. V. V. Solodovnikov, Statistical Dynamics of Linear Automatic Control Systems, London: D. Van Nostrand Co., Ltd., 1965.

41. Ya. Z. Tsypkin, Sampling Systems Theory, Vols. 1 and 2, Oxford: Pergamon Press Ltd., 1964.

42. P. D. Krut'ko, Statistical Dynamics of Sampled Data Systems, London: Iliffe Books Ltd., 1969.